INL/CON-13-29006
PREPRINT

Computational Intelligence Based Data Fusion Algorithm for Dynamic sEMG and Skeletal Muscle Force Modeling

6th International Symposium on Resilient Control Systems

Chandrasekhar Potluri
Madhavi Anugolu
Marco P. Schoen
D. Subbaram Naidu
Alex Urfer
Craig Rieger

August 2013

Computational Intelligence Based Data Fusion Algorithm for Dynamic sEMG and Skeletal Muscle Force Modeling

Chandrasekhar Potluri, Madhavi Anugolu, Marco P. Schoen, D. Subbaram Naidu, Alex Urfer
Idaho State University
Pocatello, ID
Potlchan@isu.edu, anugmadh@isu.edu, schomarc@isu.edu, naiduds@isu.edu, urfealex@isu.edu

Craig Rieger
Idaho National Laboratory
Idaho Falls, ID, USA
craig.rieger@inl.gov

Abstract — **In this work, an array of three surface Electrography (sEMG) sensors are used to acquired muscle extension and contraction signals for 18 healthy test subjects. The skeletal muscle force is estimated using the acquired sEMG signals and a Non-linear Wiener Hammerstein model, relating the two signals in a dynamic fashion. The model is obtained from using System Identification (SI) algorithm. The obtained force models for each sensor are fused using a proposed fuzzy logic concept with the intent to improve the force estimation accuracy and resilience to sensor failure or misalignment. For the fuzzy logic inference system, the sEMG entropy, the relative error, and the correlation of the force signals are considered for defining the membership functions. The proposed fusion algorithm yields an average of 92.49% correlation between the actual force and the overall estimated force output. In addition, the proposed fusion-based approach is implemented on a test platform. Experiments indicate an improvement in finger/hand force estimation.**

Keywords — Approximate Entropy, Data fusion, Fuzzy logic

I. Introduction

Investigation into the field of advanced prostheses was started after World War II [1]. Since then it has been an ongoing research topic that yielded many innovations. However, to date, there is no prosthetic device available at an affordable cost that mimics the human hand well. There are also no affordable prosthetics on the market with vibrotactile feedback [2]. In order to measure the electrical activity of the skeletal muscle force, one can utilize an invasive, needle electrode based method or a non-invasive, skin surface based technique. As a result of its simplicity, there has been a lot of research done in the field of surface Electromyographic (sEMG) based prostheses. The sEMG signal obtained from the muscle contraction can be used as a control signal for a prosthetic limb [3]. Since it is acquired from the surface of the skin, it passes through several tissue layers before reaching the skin surface and it will be influenced by many external factors, such as environmental noise and electrophysiology [4]. In order to make better use of the sEMG signal, filtering is required. There are different filtering techniques available and the authors explored an array of different filters in their previous work [5]. In particular, the half-Gaussian filter as used in [5, 6] has performed very well; however, it also poses a severe drawback: it cannot be implemented in real time. Hence, in this work, wavelet transforms are utilized to filter sEMG signals. One of the main advantages of the wavelet transform based filtering technique is that it can be implemented in real-time and is computationally relatively inexpensive.

In general, the force generated by the muscle action can be achieved by muscle activation and muscle contraction [7]. The measurement of muscle force is required in many applications such as prosthetic control, human-robot interaction, etc [8]. According to [9], force estimation based on sEMG measurements is one of the best alternatives to the commercially available force measuring sensors. There are different sEMG-force relationship models proposed by the research community. A few to name are: Hill-type models [10], cross-bridge models [11], and curve fitting methods [12]. In this work, we utilized a non-linear Wiener Hammerstein (WH) model obtained through the use of system identification [13]. This allows modeling the dynamic relationship between the sEMG and the corresponding skeletal muscle force.

Usually, sEMG data is measured by using a single sensor. However, in this work, an array of three sensors is used and the data is fused using a proposed decision-level fusion algorithm. The paper is organized as follows. The present section covers the literature review and introduction, and the next section describes the experimental set-up. These are followed by the proposed design which explains about the filtration, WH algorithms and the proposed fusion algorithm followed by the results and discussion and some conclusions are provides at the end.

II. Experimental Set-Up

Fig. 1 shows the experimental set-up used to capture sEMG and force signals. The motor points and the appropriate EMG electrode attachment points of the subject were identified by using a wet probe point muscle stimulator (Rich-Mar Corporation, model number HV 1100). The proposed fusion algorithm is developed for arbitrary number of sensors. However, for this work the utilized sensor size in relation to the motor point is too large to employ more than three sensors. The sEMG sensor at the center in Fig. 1 is at the motor point while the other two sensors are adjacent to the motor point. The sEMG signals are captured from the surface of the skin using DE 2.1 sEMG sensors with a DELSYS® Bagnoli EMG system and LabVIEW™. The sEMG and the skeletal muscle force signals are acquired simultaneously, while the test subjects are made to perform random grasping actions. The force signal is acquired by a Force Sensing Resistor (FSR). Both the sEMG signals and the corresponding skeletal muscle force are acquired at a sampling rate of 2000 samples per second. Prior to placing the sEMG sensors, the skin surface of the subject was prepared according to the International Society of Electrophysiology and Kinesiology (ISEK) protocols [14].

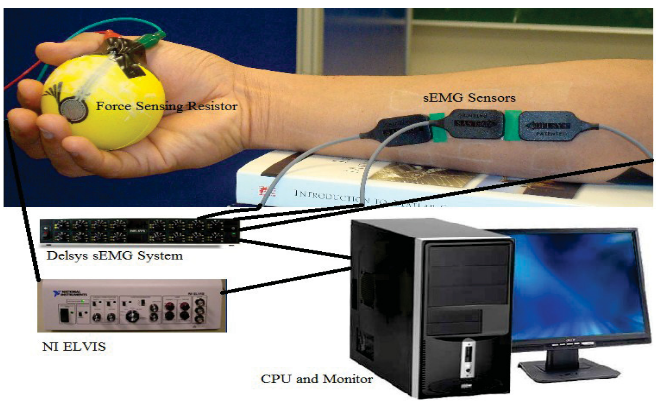

Fig. 1. Experimental Set-Up

III. PROPOSED DESIGN

Filtration:

After extracting the data from the sEMG sensors around an individual motor point, the sEMG data is filtered using a Wavelet Transform (WT) based Daubechies 44 filter at seven levels of decomposition. The single level of Discrete Wavelet Transform (DWT) is given as

$$u_{fi}[n] = \left(u_{ufi} * g_i\right)[n] = \sum_{k=-\infty}^{\infty} u_{ufi}[k]\, g_i[n-k], \tag{1}$$

where i is the corresponding sensor,

u_{ufi} is the unfiltered sEMG signal,

u_{fi} - Filtered sEMG signal,

g_i - Low-pass filter with impulse response.

$$u_{fi_{low}}[n] = \sum_{k=-\infty}^{\infty} u_{ufi}[k]\, g_i[2n-k] \tag{2}$$

$$u_{fi_{high}}[n] = \sum_{k=-\infty}^{\infty} u_{ufi}[k]\, h_i[2n-k] \tag{3}$$

where h_i - high pass filter

System Identification:

After pre-processing the data, the sEMG data $u_1(t), u_2(t)$ and $u_3(t)$ from the three sensors and their corresponding skeletal force signals are used to identify the dynamic relationship by utilizing System Identification (SI). The model structure of the linear and nonlinear dynamics of the sEMG signal and the corresponding skeletal muscle force is selected by using a Wiener-Hammerstein (WH) model.

The mathematical representation of the modeling is given by,

$$w_i(t) = f(u_i(t)), \tag{4}$$

$$\hat{x}_i(t) = \frac{B_{j,i}(q)}{F_{j,i}(q)} w_i(t-nk) + e(t), \tag{5}$$

$$\hat{y}_i(t) = h(\hat{x}_i(t)), \tag{6}$$

where (t) is the sEMG signal and $y(t)$ is the skeletal muscle force signal. f and h are nonlinear functions, $w(t)$ and $x(t)$ are internal variables, $B_{j,i}(q)$ and $F_{j,i}(q)$ are polynomials, q is the back shift operator, and $e(t)$ is the output error. The WH model structure utilizes an OE model, which is given by,

$$\hat{y}(t) = \frac{B(q)}{F(q)} u(t-nk) + e(t) \tag{7}$$

where nk is the system delay and t is time index. From (4) and (7), WH captures both the linear and non-linear dynamics of the sEMG signal.

Three WH models, M_1, M_2 and M_3 are extracted by utilizing the data from the three sensors u_1, u_2 and u_3 and their corresponding skeletal muscle force (y). With these three models, three features are computed: Approximate Entropy (AE), Relative Error (RE) and the correlation. Based on these features, a fuzzy logic inference system is designed to compute the weights of each individual model. The weights from the fuzzy logic represent the influence of each model on the estimated skeletal muscle force. The intent of the fusion is to obtain a better skeletal muscle force estimate.

Fusion Algorithm:

Step 1: Compute entropy, from a time series of data $\hat{y}_i(1), \hat{y}_i(2), \ldots \hat{y}_i(N)$ Where N - number of data points

Step 2: Fix m, an integer, and r, a positive real number. The value of m represents the length of compared run of data, and r specifies a filtering level.

Step 3: Form a sequence of vectors $x(1), x(2), \ldots x(N-m+1)$ in R^m defined by the discrete sequence of the input sEMG data $x(k) = [u(k), u(k+1), \ldots u(k+m-1)]$.

Step 4: Use the sequence $x(1), x(2), \ldots x(N-m+1)$ to construct, for each k, $1 \le k \le N-m+1$ $C_k^m(r) =$ (Number of $x(j)$ such that $d\left[x(k), x(j)\right] < r$) / $(N-m+1)$ $d\left[x, x^*\right]$ is defined as $d\left[x, x^*\right] = \max_a \left|u(a) - u^*(a)\right|$, where $u(a)$ - m scalar components of x d - represents the distance between the vectors $x(k)$ and $x(j)$.

Step 5: Define $\Phi^m(r) = (N-m+1)^{-1} \sum_{i=1}^{N-m+1} C_i^m(r)$.

The quantity $C_i^m(r)$ is the fraction of patterns of length m that resemble the pattern of the same length that begins at interval i, we define $\Phi^m(r)$ as the mean of these $C_i^m(r)$ values

Step 6: Define approximate entropy (E) as

$$E_i = \log(\Phi^m(r)) - \log(\Phi^{m+1}(r)).$$

where log is the natural logarithm, for m and r fixed as in Step 2.

Step 7: Compute Relative Error (RE) between actual force (y) and the individual WH model estimated force ($\hat{y}$)

$$\eta = \frac{\delta y}{\hat{y}_i}, \text{ where } \delta y = y - \hat{y}$$

y - Actual force from FSR

$\hat{y}$ - Individual WH model estimated force

Step 8: Compute Correlation coefficient as

$$\rho_i = \frac{\operatorname{cov}(y, \hat{y})}{\sigma_y \sigma_{\hat{y}}} = \frac{E\left[(y-\mu_y)(\hat{y}-\mu_{\hat{y}})\right]}{\sigma_y \sigma_{\hat{y}}}$$

where μ - Mean, σ - Standard Deviation

Step 9: Define the fuzzy inference system,

$$F^z = \mathit{If}\ E_i A_1^z\ \mathit{or}\ \rho_i B_1^z\ \mathit{or}\ \eta_i C_1^z\ \mathit{then}\ W^z\ \mathit{is}\ D_1^z$$

where $F^z(I = 1,2,\ldots,l)$ denotes the I^{th} fuzzy rule, $E_i(i = 1,2,\ldots,M_i)$, $\rho_i(i = 1,2,\ldots,M_i)$, $\eta_i(i = 1,2,\ldots,M_i)$, are the entropy, correlation and relative error inputs for the M_i^{th} model W^z is the output weight of the fuzzy rule F^z ,and $A_1^z(I = 1,2,\ldots,l)$is the Gaussian fuzzy membership function $B_1^z(I = 1,2,\ldots,l)C_1^z(I = 1,2,\ldots,l)$ $D_1^z(I = 1,2,\ldots,l)$ are triangular fuzzy membership functions respectively.

Step 10: Compute the fused model output $\hat{Y}_f = \sum_{i=1}^{s} W_i^z \hat{y}_i$

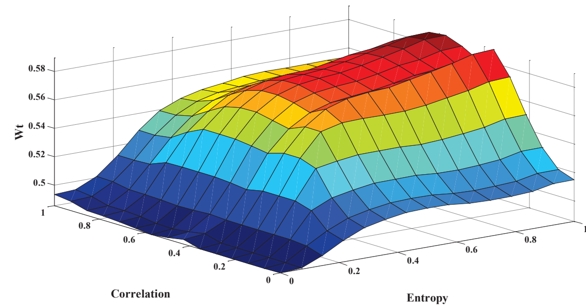

Fig. 2. Surface plot for the entropy, correlation coefficients and the corresponding weights for each sensor

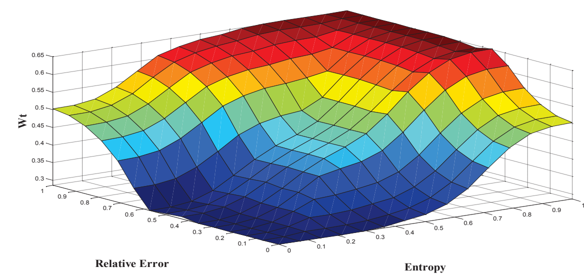

Fig. 3. Surface plot for the entropy, RE and the corresponding weights for each sensor

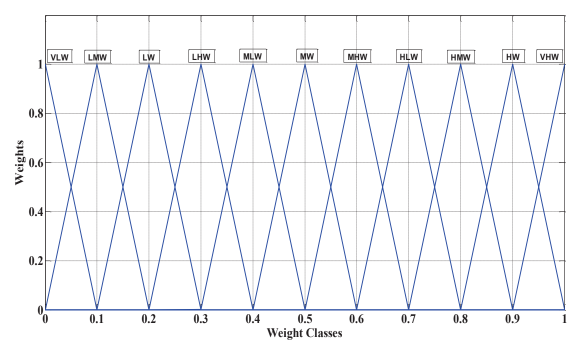

Fig. 4. Weight classes for the fuzzy inference system

Fig. 2 and 3 shows the fuzzy inference system surface plots based on entropy, RE and the correlation coefficient for each sensor. Fig. 4 shows the triangular defuzzification for the output weights of the fuzzy inference system, where VLW, LMW, LW LHW, MLW, MW, MHW, HLW, HMW, HW and VHW represents weights of the three WH models based on Entropy (E), Relative Error (RE) and the correlation.

TABLE I: MODEL BASED RESULTS AND OVERALL ESTIMATED FORCE CORRELATION COEFFICIENTS

Subjects	M_1				M_2				M_3				$\hat{Y}_f$
	η	ρ	E	W	η	ρ	E	W	η	ρ	E	W	
1	30.67	70.05	0.31	0.23	**27.4**	**72.67**	**0.17**	**0.67**	41.93	62.23	0.52	0.10	92.48
2	32.48	69.13	0.40	0.25	**26.09**	**73.24**	**0.13**	**0.72**	41.43	65.90	0.47	0.30	93.09
3	32.21	71.39	0.23	0.19	**28.71**	**74.10**	**0.19**	**0.65**	39.08	68.54	0.58	0.16	92.66
4	31.67	68.20	0.29	0.20	**27.98**	**71.89**	**0.20**	**0.63**	40.35	63.55	0.51	0.17	92.20
5	*39.53*	*61.24*	*0.55*	*0.07*	**29.55**	**73.50**	**0.18**	**0.64**	*30.92*	*70.82*	*0.27*	0.29	92.25
6	32.67	68.97	0.57	0.17	**27.60**	**71.84**	**0.19**	**0.62**	39.73	62.39	0.24	0.21	92.21
7	33.56	69.21	0.21	0.21	**28.39**	**72.54**	**0.19**	**0.61**	38.05	64.56	0.60	0.18	92.27
8	30.12	71.51	0.21	0.23	**26.05**	**70.23**	**0.15**	**0.69**	43.83	63.0	0.64	0.08	92.03
9	*42.29*	*62.93*	*0.61*	*0.06*	**26.11**	**71.47**	**0.13**	**0.73**	*31.60*	*68.31*	*0.26*	*0.21*	92.09
10	33.23	70.34	0.25	0.18	**28.92**	**72.82**	**0.17**	**0.66**	37.85	62.45	0.55	0.16	93.10
11	30.02	71.23	0.27	0.20	**27.57**	**74.30**	**0.14**	**0.75**	42.41	64.51	0.59	0.05	93.07
12	32.55	69.90	0.26	0.16	**28.39**	**73.45**	**0.18**	**0.64**	39.06	61.57	0.56	0.20	92.15
13	31.11	68.70	0.28	0.14	**27.90**	**71.32**	**0.17**	**0.68**	40.99	62.90	0.55	0.18	92.30
14	33.03	70.25	0.25	0.19	**26.74**	**71.64**	**0.15**	**0.73**	40.23	61.36	0.52	0.08	93.17
15	30.21	68.97	0.36	0.17	**27.13**	**70.16**	**0.11**	**0.77**	42.66	63.56	0.53	0.06	92.28
16	*41.05*	*58.76*	*0.59*	*0.10*	**26.50**	**72.96**	**0.14**	**0.73**	*32.45*	*69.92*	*0.27*	*0.17*	92.91
17	30.78	69.11	0.39	0.22	**27.93**	**71.67**	**0.11**	**0.76**	41.29	62.21	0.50	0.02	92.17
18	30.55	69.62	0.28	0.13	**28.45**	**70.93**	**0.18**	**0.64**	41.00	63.60	0.54	0.23	92.31

η - % Relative Error, ρ - % Correlation, E - Approximate Entropy

IV. RESULTS AND DISCUSSION

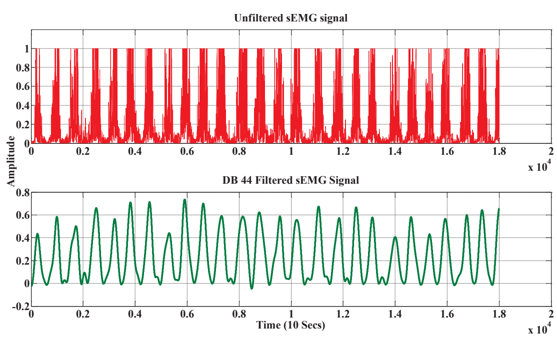

Fig. 5. Unfiltered sEMG signal and the wavelet transform based DB 44 filter at seven levels of decomposition

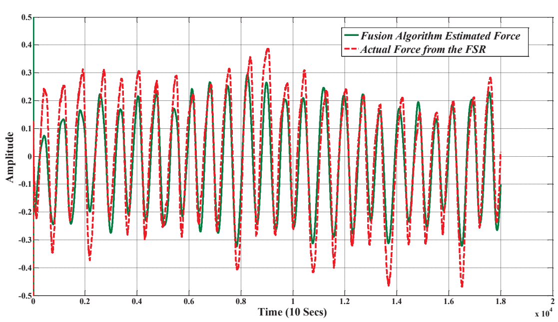

Fig. 6. Fusion algorithm estimated force and the actual force from the FSR plotted together

Fig. 5 Shows the unfiltered sEMG signal and the wavelet transform based DB 44 filter at seven levels of decomposition. Fig. 6 shows the fusion algorithm estimated force ($\hat{Y}_f$) and the actual force (y) from the FSR plotted together.

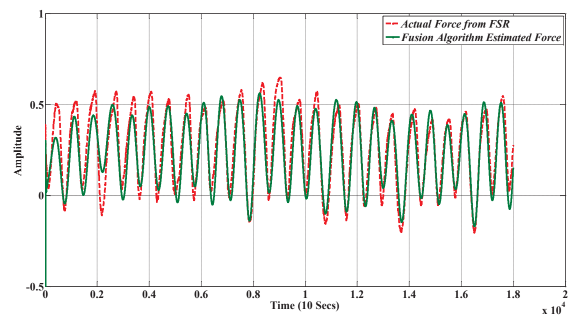

Fig. 7. Fusion algorithm estimated force and the actual force from the FSR plotted together for a different subject

From Fig. 6, it can be inferred that fusion algorithm estimated force is following the same trend as the actual force from the FSR. Fig. 7 shows the validation of the fusion algorithm with a different test subject's sEMG data.

Table I provides a comparison of the entropy, RE and the correlation coefficients between actual force along with the individual WH model and fusion algorithm estimated forces for the 18 different subjects. The models M_2 constructed from the sensor data u_2 - which located right on the motor unit – is yielding a better correlation coefficient and a lower RE between the actual force and the WH model estimated force.

Also, the entropy of M_2 is very low for all the subjects when compared to other models M_1 and M_3. Therefore, by the definition of entropy from the information theory, it is evident that M_2 is more predictable and has more information than the other two models. It is also evident from Table I that the weights computed by the fuzzy inference system are following the same trend, giving the highest weightage to M_2. Therefore from step 10 of the fusion algorithm, the estimated force from M_2 is given the highest weightage. It is evident from the last column of Table I that the fusion algorithm estimated force ($\hat{Y}_f$) is showing a marked improvement in terms of correlation with the actual force when compared with individual WH model estimated forces for all the subjects.

It can also be inferred from Table I that, M_1 is giving the second highest weightage followed by M_3 except for subjects 5, 9 and 16. It is interesting that all the three features RE, AE and correlation are showing better performance for M_3 over M_1 for these three subjects. Therefore, the proposed fuzzy logic inference system is able to adapt to this trend.

V. CONCLUSION AND FUTUREWORK

In this paper, a Wavelet with Daubechies 44 based filter is implemented for the use of filtering sEMG data. The filtering approach provides better performance compared to the other filters used by the authors in their previous work [5, 15]. An added benefit for using the proposed Wavelet based filter is the ease of implementation for real time use, which is not possible for the half Gaussian filter. Time domain nonlinear WH modeling technique is utilized to characterize the dynamics of the sEMG/skeletal muscle force data. A computational intelligence based fusion algorithms is proposed for the sEMG sensor data fusion for the better estimation of the skeletal muscle force from Table I [5, 16] and also make the sEMG/skeletal muscle force models resilient to sensor miss alignment.

Although better individual models can be inferred using SI under perfect conditions, the proposed fusion algorithms improves the predicted force estimate consistently. The influence of cross talk can be reduced by using filtering. From the results, it is clear that the proposed model fusion algorithm works well for the sEMG-force relationships. The proposed fusion algorithm is giving the highest correlation of 93.10% between fusion algorithm estimated force ($\hat{Y}_f$) and the actual force (y) compared to the individual WH models skeletal muscle force estimation. This implies that the fusion algorithm is improving the overall output. The proposed fusion algorithm is computationally efficient when compared to other algorithms that were previously developed by the authors [15, 16].

The sEMG based finger force models (nonlinear WH) are constructed based on the normal limb sEMG and a force measurement. It gives the dynamic relationship between sEMG and skeletal muscle force. These dynamic models can be mapped to an amputee who has a variable amount of residual musculature, varying levels of atrophy, and an unknown force output. Recalibrating the models with the sEMG data from the amputee can be accomplished by using an existing limb or standard force models (in case of multiple limb amputation). This design can also be extended to above elbow amputations by approximating the sEMG data from the biceps and triceps.

Future work will address the real-time implementation of this algorithm. From the results it is also evident that this algorithm can be utilized for uncertainty analysis and anomaly detection. It will be very interesting to apply this algorithm for uncertainty analysis of a much larger sEMG array sensor.

ACKNOWLEDGMENT

This research was sponsored by the U.S. Department of the Army, under the award number w81xwh-10-1-0128 awarded and administered by the U.S. Army medical research acquisition activity, 820 Chandler Street, Fort Detrick MD 21702-5014. The information does not necessarily reflect the position or the policy of the government, and no official endorsement should be inferred. For purposes of this article, information includes news releases, articles, manuscripts, brochures, advertisements, still and motion pictures, speeches, trade association proceedings, etc. Further the technical help from Dr. Steve Chiu and Dr. Jim Creelman is greatly appreciated.

REFERENCES

[1] E. F. Murphy and A.B. Wilson. Limb Prosthetics and orthotics. In M. Clynes and J.H. Milsum, editors, Biomedical Engineering Systems, Pages 489-549. McGraw-Hill, New York, NY, 1970

[2] D.S. Naidu and C.-H. Chen, "Control Strategies for Smart Prosthetic Hand Technology: An Overview", Book Chapter 14, to appear in a book titled, Distributed Diagnosis and Home Healthcare (D2H2): Volume 2, American Scientific Publishers, CA, January 2011.

[3] H.B. Evans, Z. Pan, P.A. Parker and R.N. Scott, "Signal processing for proportional myoelectric control", IEEE Trans. Biomed, Eng., Vol. BME-31, pp-207-211, Feb 1984.

[4] Y. Huang, H. B. Englehart, B. Hudings, and A.D.C. Chan, "A gaussian mixture model based classification scheme for myoelectric control of powered upper limb prosthese," IEEE Trans. Biomed. Eng., vol-52, no. 11, pp. 1801-1811, Nov. 2005.

[5] Chandrasekhar Potluri, Madhavi Anugolu, Steve Chiu, Alex Urfer, Marco P. Schoen, D. Subbaram Naidu, " Fusion of Spectral Models for Dynamic Modelling of sEMG and Skeletal Muscle Force," 34th Annual International Conference of IEEE EMBS, san Diego, CA, USA, Aug 28-Sep 1, 2012.

[6] T.D. Sanger, "Bayesian Filtering of Myoelectric Signals," J. Neurophysiol 97: 1839-1845, 2007, Frist Published 20, Dec 2006.

[7] F. Zajac, "Muscle and tendon: properties , models scaling and application to biomechancis and motor control," Crit. Rev. Biomed. Eng., vol. 17, no. 4, pp.359-411, 1989.

[8] D. Staudemann, K. Roeleveld, D. Stegeman, and J. van Dieen, " Methodological aspects of sEMG recordings for force estimation- A tutorial and review," Journal of Electromyography and Kinesiology, vol.20, pp. 375-397, 2010

[9] Javad Hashemi, Keyvan Hashtrudi-Zaad, Evelyn Morin, and Parvin Mousavi, "Dynamic Modoeling of EMG-Force Relationship using paralle cascade Identification, 32nd Annual International Conference of the IEEE EMBS , Buenos Aires, Argentina, Aug 31- Sep 4, 2010.

[10] F.Zajac, "Muscle and tendon: Properties, models, scaling and application to biomechanics ans motor control," Crit. Rev. Biomed. Eng., vol.17, no. 4, pp.359-411, 1989

[11] A.Huxley, "Muscle structure and theories of contraction," Process in biophysics and biophysical chemistry, vol.7, p.255, 1957.

[12] E. Clancy, O. Bida, and D. Rancout, “Influence of advanced electromyogram amplitude processors on EMG-to-torque estimation during constant-posture, force –varying contractions,” Journal of Biomechanics, vol.39, no. 14, pp. 2690-2698, 2006.

[13] Parmod Kumar, Chandrasekhar Potluri, Anish Sebastian, Steve Chiu, Alex Urfer, D. S. Naidu, and Marco P. Schoen, “Adaptive Multi Sensor Based Nonlinear Identification of Skeletal Muscle Force,” WSEAS Transactions on Systems, Issue 10, Volume 9, October 2010, pp. 1051-1062, 2010

[14] http://www.isek-online.org/standards_emg.html.

[15] Anugolu Madhavi, Sebastian Anish, Parmod Kumar, Marco P. Schoen, Alex Urfer and D. S. Naidu, “ Surface EMG array sensor based model fusion usin Bayesian approaches for Prosthetic Hans”, Proceeding of the Dynamic Systems and Control Conference, Hollywood, CA, October 2009.

[16] Chandrasekhar Potluri, Parmod Kumar, Madhavi Anugolu, Alex Urfer, Steve Chiu, D. Subbaram Naidu, and Marco P. Schoen, *“Frequency Domain Surface EMG Sensor Fusion for Estimating Finger Forces,”* 32nd Annual International Conference of the IEEE Engineering in Medicine and Biology Society, Buenos Aires, Argentina, Aug. 31 – Sept. 4, 2010.